

# Movable Cross-linking in Adhesives: Superior Stretching and Adhesion Properties via a Supramolecular Sliding Effect

Mo-Beom Yi, Tae-Hyung Lee, Gi-Yeon Han, Hoon Kim, Hyun-Joong Kim,\* Youngdo Kim, Han-Sun Ryou, and Dong-Un Jin



Cite This: *ACS Appl. Polym. Mater.* 2021, 3, 2678–2686



Read Online

ACCESS |



Metrics & More



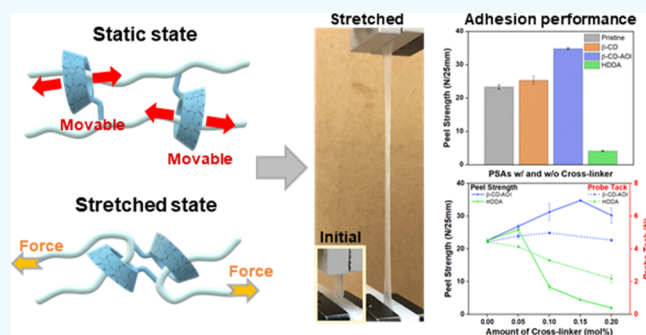
Article Recommendations



Supporting Information

**ABSTRACT:** Cross-linking is an essential element in enhancing polymers' mechanical properties in adhesives, elastomers, and hydrogels. However, covalent cross-linking introduces a trade-off relationship between cohesive interactions and chain mobility of polymers, thus restricting stretching and adhesion properties. Herein, a supramolecular cross-linker is synthesized by giving an acrylate functional group to  $\beta$ -cyclodextrin. The supramolecular cross-linker shows a sliding effect in polymers with a threaded structure via the cavity of  $\beta$ -cyclodextrin. Compared to conventional adhesives, the supramolecular cross-linked adhesives exhibit exceptional stretching and adhesion properties because of their retained chain mobility from the sliding effect. This approach for movable cross-linking could widen adhesives' application by overcoming the restrictions of conventional cross-linking.

**KEYWORDS:** sliding effect, movable cross-linker, supramolecular chemistry, cyclodextrins, non-covalent interactions



## 1. INTRODUCTION

In developing technologies for the Industry 4.0, advanced polymeric materials with toughness, stretching, and durability have gained considerable attention.<sup>1–4</sup> The mechanical properties of polymers are based on various factors that include the composition of monomers, molecular weight, and types of cross-linkers. Such factors should be controlled delicately to assign appropriate properties for polymers. A cross-linker is identified as one of the most critical elements among them, generating covalent bonds between polymer chains to increase cohesive interactions.<sup>5,6</sup> Polymers can endure much greater forces from strain or pressure using cross-linkers. However, the covalent bonds cause a trade-off relationship between mechanical strength and chain mobility in polymers, and this limitation is distinctive in adhesives. A high concentration of cross-linking causes more strong cohesion in adhesives but restricts the chain mobility simultaneously.<sup>7–9</sup> The hindered chain mobility weakens the adhesion properties, affecting the wettability and interfacial interactions.<sup>10,11</sup> Therefore, the trade-off relationship between cohesion and adhesion is a crucial obstacle to obtaining advanced adhesives.

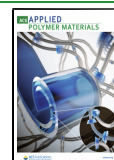
Supramolecular materials,<sup>12,13</sup> which have noncovalent interactions including hydrogen bonds,<sup>14,15</sup>  $\pi$ - $\pi$  interactions,<sup>16</sup> and host-guest interactions,<sup>17,18</sup> have been receiving enormous attention because of their unusual functionalities. Supramolecular materials used in hydrogels,<sup>19–21</sup> elastomers,<sup>22,23</sup> and coatings<sup>5</sup> have exhibited outstanding character-

istics such as self-assembly,<sup>24</sup> self-healing,<sup>25–28</sup> and switchable mechanical properties.<sup>29</sup> Adhesives with supramolecular interactions also have been focused on, recently, to give special characteristics.<sup>30–32</sup> Hydrogen bonds were introduced to enhance peel strength<sup>33,34</sup> and give a selective adhesion property.<sup>35</sup> Underwater adhesion<sup>16</sup> and reversible adhesion<sup>20,36</sup> were achieved through host-guest interactions with cucurbituril and cyclodextrins. Although the aforementioned supramolecular adhesives obtained outstanding characteristics, they are not free from the trade-off relationship, which needs compensation (e.g., chain mobility) to increase the cohesive force. Hence, a novel strategy to overcome the limitation of conventional cross-linking is strongly required. Recently, polyrotaxane has got attention for its sliding effect, which results in a superior enhancement in mechanical properties for polymers.<sup>37,38</sup> The cyclodextrins in polyrotaxane move along the polymer chain, and this sliding effect lowers the stress and increases the stretching property of the polymer. Also, this movable cross-linking system might be a solution for the limitation of the covalent cross-linking in adhesives.

**Received:** February 18, 2021

**Accepted:** April 8, 2021

**Published:** April 22, 2021



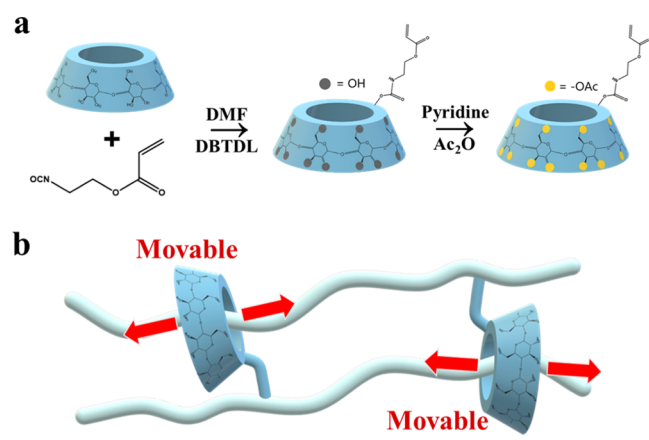
In this study, we synthesized a supramolecular cross-linker by attaching an acrylate functional group to  $\beta$ -cyclodextrin ( $\beta$ -CD) through a urethane reaction. This supramolecular cross-linker showed a sliding effect via the threaded structure onto acrylate polymers without the need for polyrotaxane synthesis.<sup>39</sup> Adhesives with the supramolecular cross-linker exhibited outstanding stretching and adhesion properties, showing exceptional chain mobilities despite the enhanced cohesive interaction. The limitation of conventional cross-linking has been overcome by the sliding effect of the supramolecular movable cross-linker.

## 2. EXPERIMENTAL SECTION

**2.1. Materials.** Butyl acrylate (BA), 2-ethylhexyl acrylate (2-EHA), dibutyltin dilaurate, dodecyl acrylate, and 1,6-hexanediol diacrylate (HDDA) were purchased from Sigma-Aldrich (USA). 2-Hydroxyethyl acrylate, acetic anhydride, and pyridine were purchased from Samchun (Korea).  $\beta$ -CD was purchased from TCI (Japan). 2-Isocyanatoethyl acrylate (AOI) was purchased from Showa Denko (Japan). Acetone, dimethylformamide (DMF), and deionized (DI) water were purchased from Daejung (Korea). The Omnirad 1173, a photoinitiator (PI), was purchased from IGM (Netherlands).

**2.2. Synthesis of a Supramolecular Movable Cross-Linker.** The movable cross-linker, named  $\beta$ -CD-AOI, was synthesized by the following steps (Scheme 1).<sup>39</sup>  $\beta$ -CD (8.63 g, 7.60 mmol) was

**Scheme 1. Illustration of the Supramolecular Movable Cross-Linker; (a) Synthetic Procedure of the Supramolecular Cross-Linker; (b) Movable Effect of the Supramolecular Cross-Linker via Threading onto Polymer Chains**



dissolved in DMF (50 mL) under a nitrogen atmosphere. After complete dissolution, dibutyltin dilaurate (40  $\mu$ L) was added to the solution as a catalyst for the urethane reaction. Then, one equivalent amount of AOI (1.07 g, 7.60 mmol) was added dropwise. The mixture was stirred for 1 h at room temperature (RT) and continued for 4 h at 40  $^{\circ}$ C. Then, the solution was poured into cold acetone (400 mL) to precipitate the product. The product was dissolved in DI water (10 mL) and precipitated again with acetone (200 mL). This procedure was repeated several times to remove unreacted materials and DMF. The final product was dried at RT in a vacuum oven overnight (yield: 68.7%, 6.65 g). The urethane reaction was characterized by the Fourier transform infrared (FT-IR) spectrum (Figure S1). The average number of AOI substituted to  $\beta$ -CD was confirmed to be one by the NMR spectrum (Figure S3), and the mass measurements of  $\beta$ -CD-AOI were performed using a matrix-assisted laser desorption ionization time-of-flight (MALDI-TOF) mass spectrometer (Figure S5).

The synthesized  $\beta$ -CD-AOI was per-acetylated to get miscibility with acrylic monomers.<sup>25</sup>  $\beta$ -CD-AOI (9.31 g, 7.3 mmol) and acetic

anhydride (85 g, 830 mmol) were dissolved in pyridine (500 mL). The solution was stirred for 12 h at 55  $^{\circ}$ C. After the reaction, methanol (35 mL) was added to the solution dropwise and cooled with an ice bath. The solution was then poured into DI water (1.5 L), and the precipitate was filtered and washed using DI water (150 mL) three times. The final product was dried under vacuum overnight (yield: 84.1%, 12.99 g). The acetylation process was confirmed by the FT-IR spectrum (Figure S2) and the NMR spectrum (Figure S4). All the supramolecular materials ( $\beta$ -CD,  $\beta$ -CD-AOI) in this study were used after the acetylation process.

**2.3. Preparation of Elastomers.** The acrylate elastomers were prepared to test the movable cross-linking effect of  $\beta$ -CD-AOI. 0.5, 0.7, or 1.0 mol % cross-linker (HDDA or  $\beta$ -CD-AOI) was dissolved in acrylic monomers (BA, 2-EHA), and 0.2 mol % of PI (Omnirad 1173) was added to the solution. All the amounts of additives were calculated with respect to the total monomer concentration. The mixture was sonicated for 30 min and poured into a Teflon mold (10  $\times$  70  $\times$  1 mm). The samples were then irradiated with a UV light-emitting diode (LED) lamp (intensity = 30 mW/cm<sup>2</sup>) for 5 min.

**2.4. Preparation of Pressure-Sensitive Adhesives.** The pressure-sensitive adhesives (PSAs) were prepared to characterize the change of chain mobility with the movable cross-linking. For the preparation of PSAs, proper viscosity of the coating solution should be provided to prevent the flow of the solution. Therefore, we prepared a pre-polymer to get an appropriate viscosity of the coating solution. The acrylic monomers (BA, 2-EHA) and PI (Omnirad 1173) were mixed in a three-neck flask equipped with a stirrer, thermometer, and a UV curing system (SP-9, USHIO). The components' ratio was 90, 10 mol % for BA, 2-EHA, and 0.2 mol % of PI was added with respect to the total monomer concentration. The mixture was irradiated by UV light (30 mW/cm<sup>2</sup>) under a nitrogen atmosphere with mechanical stirring for 1 min. The synthesized pre-polymer was a random copolymer, and its molecular weight was characterized by gel permeation chromatography ( $M_n$ : 751 kDa,  $M_w$ : 1347 kDa, and PDI: 1.79). The weight ratio of the polymer in the pre-polymer (10.1 wt %) was characterized by thermogravimetric analysis (Figure S6).

**2.5. Characterization.** The cross-linker (HDDA or  $\beta$ -CD-AOI) was added to the pre-polymer with an additional PI (0.2 mol %). Then, the mixture was coated on a silicone release film by a film applicator (60  $\mu$ m-thickness). The coated film was irradiated by a UV LED lamp (intensity = 30 mW/cm<sup>2</sup>) for 1 min.

The IR spectra were measured using a FT-IR spectrometer (Nicolet iS20, Thermo Fisher Scientific).

The <sup>1</sup>H NMR, <sup>13</sup>C NMR, and nuclear Overhauser enhancement spectroscopy (NOESY) [two-dimensional (2D) NMR] spectra were recorded at a 600 MHz NMR spectrometer (AVANCE 600, Bruker) at 25  $^{\circ}$ C. All NMR measurements used dimethyl sulfoxide (DMSO-*d*<sub>6</sub>) as the solvent and tetramethylsilane as the internal standard ( $\delta$  = 0 ppm). In 2D NMR, the pBA- $\beta$ -CD-NT (nonthreaded compound) was prepared through the polymerization of BA (819 mg, 6.4 mmol) and dodecyl acrylate (1.6 mg, 0.0068 mmol) with Omnirad 1173 (2.1 mg, 0.013 mmol) followed by the addition of the acetylated  $\beta$ -CD (762 mg, 0.34 mmol).<sup>35</sup> The dodecyl acrylate was included as a blocking agent for the threading after polymerization. A UV LED lamp (30 mW/cm<sup>2</sup>) was used for 5 min during the polymerization process. On the other hand, the acetylated  $\beta$ -CD was mixed in the acrylate monomers before the polymerization process to prepare pBA- $\beta$ -CD-T (threaded compound).

The mass measurements were performed using a MALDI-TOF (TOF/TOF 5800 system, AB Sciex).  $\beta$ -CD-AOI was dissolved in DI water, and 2,5-dihydroxy-benzoic acid was used as a matrix.

The small-angle X-ray scattering (SAXS) profile was characterized by an X-ray scattering spectrometer (Xeuss 2.0, Xenocs). The distance between the sample and the detector was 500 mm, and the irradiation time was 300 s. Cu K $\alpha$  radiation ( $\lambda$  = 1.54056  $\text{\AA}$ ) was used with a diffractometer operating at 50 kV and 0.6 mA. All SAXS measurements were performed at RT.

The tensile tests of elastomers were conducted using a texture analyzer (TAXTplus, Stable Micro Systems) with a 6 mm/min

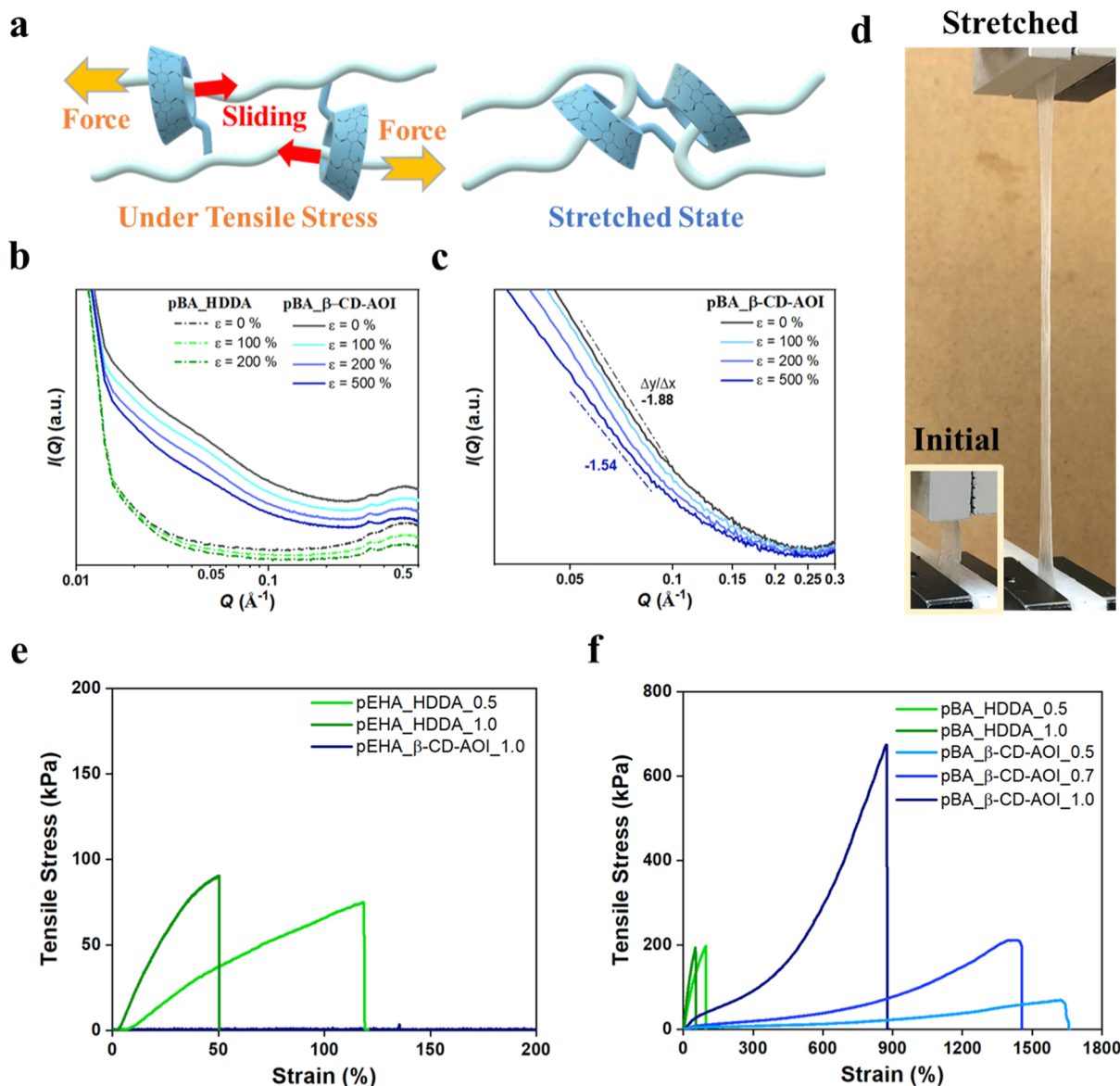


**Figure 1.** Mechanical properties of elastomers. (a) Stretched state of pBA-β-CD-AOI under tensile stress. (b,c) Scattering profiles from SAXS analysis under an uniaxial stretching process for the elastomers. The concentration of the cross-linker was 0.3 and 1.0 mol % for pBA\_HDDA and pBA\_β-CD-AOI, respectively. The one-dimensional (1D) scattering profiles were shifted vertically for a better comparison. (d) Photos of pBA\_β-CD-AOI at initial and stretched states. Stress-strain curves of (e) pEHA and (f) pBA with two cross-linker types at a 6 mm/min strain rate. The concentration of the cross-linker was 0.5, 0.7 or 1.0 mol %.

deformation rate at 25 °C. The elastomers were cut to 15 mm length for the tensile tests.

The gel content of elastomers was calculated by swelling in toluene for 24 h followed by drying in an oven at 80 °C for 24 h.

The peel and probe tack tests were conducted using a texture analyzer (TA.TX.plus, Stable Micro Systems) at 25 °C. The peel strength was measured with a 300 mm/min cross-head rate at an angle of 180°. The 100 μm polyethylene terephthalate film was used as a backing film, and the PSAs were attached to a stainless steel substrate. The film was then pressed twice with a 2 kg roller and dwelled for 20 min before the peel tests. The probe tack was measured with a 5 mm stainless steel cylinder probe at a constant detaching rate of 10 mm/s after a 100 g/cm<sup>2</sup> force with 1 s contact time. All the characterizations were repeated three times, and the average values were noted.

The rheological properties were measured using a rheometer (MCR 302, Anton Paar Ltd.). A disposable aluminum round plate of 8 mm diameter was used with a gap of 100 μm. The shear rate was 0.1–100 rad/s, and the temperature range was –40 to 70 °C with a

heating rate of 10 °C/min. All the tests were conducted by 1.0% strain. The rheological tests' specimens were prepared with a thickness of 100 μm, and they were irradiated with a UV LED lamp (intensity = 30 mW/cm<sup>2</sup>) for 2 min. All the other procedures were the same as the PSAs, which were prepared before.

The lap shear tests and stress relaxation properties were measured using a dynamic mechanical analyzer (Q800, TA Instruments) equipped with a tension clamp at 25 °C. The specimens were the same as the rheological tests, and they were attached to a poly(methyl methacrylate) substrate (20 × 6 mm) with 10 × 6 mm of adhesion area. For the lap shear test, a shear force was applied to the specimen with a ramp of 1 N/min. For the stress relaxation test, a tensile strain was applied to the specimens so that the adhesives between the substrates take a 100% shear strain. The constant shear strain was applied for 10 min, and the stress at the specimen was measured.

The glass-transition temperature was characterized by differential scanning calorimetry (DSC, Q200, TA Instruments). An aluminum pan and lid were used with 7–10 mg of PSAs. The specimens were heated from –80 to 50 °C at a constant heating rate of 10 °C/min.

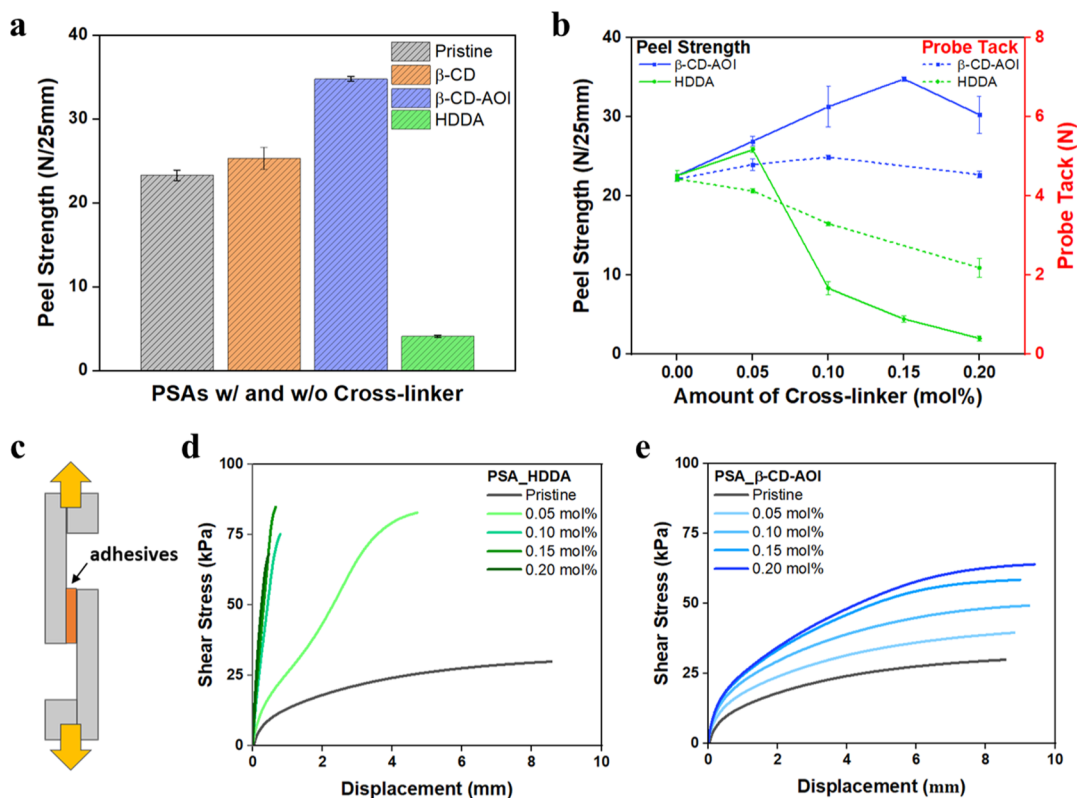


**Figure 2.** Adhesion performances of PSAs. (a) Peel strengths of PSAs with or without a cross-linker (0 or 0.15 mol %). (b) Peel strengths and probe tack data for PSAs with various concentrations of HDDDA and  $\beta$ -CD-AOI. The tests were repeated three times, and the results were averaged. (c) Scheme of the lap shear test for PSAs. Displacement–stress curves (shear) for PSAs with (d) HDDDA and (e)  $\beta$ -CD-AOI. The cross-linker concentration was 0.05–0.20 mol %.

### 3. RESULTS AND DISCUSSION

**3.1. Sliding Effect of the Supramolecular Cross-Linker in Acrylate Polymers.** A supramolecular cross-linker was prepared by attaching the acrylic functional group to  $\beta$ -CD ( $\beta$ -CD-AOI). We prepared acrylic elastomers using the supramolecular cross-linker to clarify a sliding effect from a threaded structure between the cross-linker and polymer chains (Figure 1a). BA and 2-EHA were chosen as base monomers to obtain soft elastomers because of their low-glass-transition temperature ( $T_g$ ).<sup>40</sup> However, the monomers' side groups are significantly different in size, affecting the threaded structure formation. In a simplified calculation, the side group of 2-EHA (7.58 Å) is bulkier than BA (5.07 Å) (Figure S7). Therefore, we reasoned that BA would make better threading with  $\beta$ -CD by its smaller pendant group than the cavity of  $\beta$ -CD (6.0 Å). HDDA was used as a conventional cross-linker for the comparison of the supramolecular cross-linker.

We performed 2D NMR (NOESY) analysis, which reveals the resonance signal of hydrogen atoms by the nuclear Overhauser effect, to investigate the threading of the supramolecular cross-linker onto poly(BA) (pBA) (Figure S8). The NOESY spectra of pBA- $\beta$ -CD-NT (nonthreaded) presented clear signals between the side group of BA and  $\beta$ -CD ( $C_1H$  to  $C_6H$ ). The signals might originate from a host–guest interaction with the side group (*n*-Bu) of pBA, which has an association effect for  $\beta$ -CD (association constant,  $K_a < 10 M^{-1}$ ).<sup>24</sup> However, the spectra of pBA- $\beta$ -CD-T (threaded) presented a disappearance of signals between the side group of pBA and  $\beta$ -CD, showing signals between the backbone chain of pBA and  $\beta$ -CD. The difference in NOESY NMR would be

proof for the threading of  $\beta$ -CD onto the pBA backbone. Also, the existence of threading might be a prerequisite for the sliding effect of  $\beta$ -CD-AOI in polymers.

A SAXS analysis was conducted to identify the sliding effect of the supramolecular cross-linker. Elastomers were prepared with BA and EHA monomers using HDDDA and  $\beta$ -CD-AOI as the cross-linker. However, pEHA- $\beta$ -CD-AOI, unlike other elastomers, did not show any cross-linking effect (Figure S9). It might be caused by the large side group size of EHA, hindering the threading of  $\beta$ -CD-AOI onto polymer chains. The limitation of threading was also confirmed by the lower gel content of pEHA- $\beta$ -CD-AOI (3.0%) compared to pBA- $\beta$ -CD-AOI (76.2%) (Table S1). Besides, the  $\beta$ -CD without the AOI attachment did not exhibit any cross-linking effect with 1.8% gel content for pBA. Therefore, we could conclude that  $\beta$ -CD-AOI exclusively acts as a cross-linker for the suitable monomer. pBA\_HDDA and pBA- $\beta$ -CD-AOI were investigated with SAXS, and the amount of the cross-linker was 0.3 mol % (HDDA) and 1.0 mol % ( $\beta$ -CD-AOI) to obtain proper stretchability. A core circle and halo were shown for both pBA\_HDDA and pBA- $\beta$ -CD-AOI in the 2D SAXS images (Figure S10). However, the core circle for pBA- $\beta$ -CD-AOI was larger compared to pBA\_HDDA. The higher scattering intensity might originate from  $\beta$ -CD in pBA- $\beta$ -CD-AOI, and the halo would be a result of the irregular orientation of the acrylic polymer chains in the elastomers.<sup>41,42</sup> We could also verify the difference between pBA\_HDDA and pBA- $\beta$ -CD-AOI through the 1D scattering profiles (Figure 1b,c). The scattering profiles,  $I(Q)$ , showed an apparent increase with pBA- $\beta$ -CD-AOI compared to pBA\_HDDA. The higher

scattering for pBA- $\beta$ -CD-AOI could indicate that  $\beta$ -CD-AOI would make a specific domain in the elastomer compared to the covalently cross-linked elastomer (pBA\_HDDA), which might show a considerably similar structure with pBA. Also, pBA\_HDDA with uniaxial stretching ( $\sim 200\%$ ) showed a negligible change in the scattering profile. On the other hand, pBA- $\beta$ -CD-AOI might form randomly oriented domains for the unstretched state, showing a slope of  $-1.88$  in a high- $Q$  regime. With an elongation of  $\sim 500\%$ , the slope of pBA- $\beta$ -CD-AOI showed a clear change in the region ( $-1.88$  to  $-1.55$ ), which could be related to a more oriented structure.<sup>41</sup> Also, the azimuthal analysis presented an anisotropic change with the stretching of pBA- $\beta$ -CD-AOI (Figure S10c,d). From the SAXS data, we could reason that  $\beta$ -CD-AOI would be slid in the polymer chains at the stretching process and stacked with other  $\beta$ -CD-AOI making more oriented domains in elastomers.

The stress-strain curves were obtained from tensile tests with varying amounts of the cross-linker (Figure 1d-f). The pEHA elastomer with HDDA showed elongation at break for 118% (pEHA\_HDDA\_0.5) and 50% (pEHA\_HDDA\_1.0) (Figure 1d). The tensile strengths of pEHA\_HDDA\_0.5 and pEHA\_HDDA\_1.0 were 76 and 92 kPa, respectively. The low mechanical properties of pEHA\_HDDA might originate from covalent cross-linking, which cannot dissipate the applied energy by their strict bonds.<sup>43</sup> Also, the results for pBA\_HDDA showed a similar tendency. The pBA\_HDDA\_0.5 and pBA\_HDDA\_1.0 showed comparable tensile strengths ( $\sim 195$  kPa) and elongation at break for 67 and 36%, respectively (Figure 1f). However, the pBA with the supramolecular cross-linker ( $\beta$ -CD-AOI) showed exceptional mechanical properties. The elongation at break was dramatically increased to 1632% for pBA- $\beta$ -CD-AOI\_0.5, 1440% for pBA- $\beta$ -CD-AOI\_0.7, and 872% for pBA- $\beta$ -CD-AOI\_1.0. Furthermore, the tensile strength of pBA- $\beta$ -CD-AOI\_1.0 reached 674 kPa, which was 250% larger compared to pBA\_HDDA\_1.0. The fracture energy of pBA- $\beta$ -CD-AOI\_1.0 ( $1.98$  MJ m<sup>-3</sup>) was 30 times higher than pBA\_HDDA\_1.0 ( $59$  kJ m<sup>-3</sup>). These superior tensile strengths and fracture energies may result from the sliding effect, which dissipates the applied energy efficiently.

The pBA- $\beta$ -CD-AOI was investigated with cyclic tensile tests to verify the stretchability. We stretched pBA- $\beta$ -CD-AOI\_1.0 to 200, 400, and 600 strain % for 20 cycles, and the elastomer was positioned statically for the recovery of deformation (Figure S11). The elastomer showed some hysteresis during the cycles with decreased toughness and Young's modulus, and the elastomer was deformed to a certain degree after the tests. However, the elastomer showed considerable recovery behavior after a 30 min relaxation period. The recovery of the elastomer might originate from the relaxation of the  $\beta$ -CD-AOI, which might be stacked in the stretched state by the sliding effect.

**3.2. Adhesion Properties of PSAs with a Supramolecular Sliding Effect.** PSAs are a class of adhesives that use light pressure to initiate adhesion without chemical reactions.<sup>44</sup> The PSAs should have an adequate elastic modulus and softness to exhibit adhesion properties.<sup>45,46</sup> We applied the  $\beta$ -CD-AOI to PSAs to characterize the sliding effect on adhesion properties by 180° peel, probe tack, and lap shear tests (Figures 2 and S12). The PSAs without a cross-linker showed an average peel strength of 23.27 N/25 mm, and the PSA- $\beta$ -CD devoid of the AOI attachment also showed a

comparable peel strength (25.29 N/25 mm). Surprisingly, the peel strength of the PSA- $\beta$ -CD-AOI was increased to 34.77 N/25 mm, which was 49.4% larger than PSA\_pristine. We could see that unmodified  $\beta$ -CD does not participate in a cross-linking of PSAs, showing little change in adhesion properties compared to  $\beta$ -CD-AOI. In the case of PSA\_HDDA, it showed a drastic decrease of the peel strengths (4.07 N/25 mm). We conducted additional peel and probe tack tests to determine the reasons for the difference in adhesion properties between  $\beta$ -CD-AOI and HDDA (Figure 2b). The peel strength of PSA\_HDDA was improved slightly at 0.05 mol % (25.86 N/25 mm) but showed a crucial decrease over the concentrations. Simultaneously, the tackiness has declined with the increased amount of HDDA. The decline of tackiness outweighs the improved cohesive interactions with an over-added cross-linker, causing deteriorated peel strengths. Likewise, the cross-linker amount should be limited to a specific concentration by decreased peel strengths for conventional PSAs. This trade-off relationship would be a significant obstacle to establish superior adhesion properties. However, the sliding effect from  $\beta$ -CD-AOI could make the PSAs free from the trade-off relationship. The addition of  $\beta$ -CD-AOI, as a movable cross-linker, enhanced the peel strength of PSAs up to 34.79 N/25 mm (0.15 mol %). As we could not find a significant change with  $\beta$ -CD, the enhancement of the peel strength from  $\beta$ -CD-AOI might originate from the formation of cross-linking in PSAs. Meanwhile, the tackiness of PSAs was maintained at the original strength ( $\sim 4$  N) despite the addition of the cross-linker. The tackiness is strongly related to the mobility of polymer chains, so we could reason that  $\beta$ -CD-AOI did not hinder the mobility though it increased the cohesive interaction by cross-linking. The sliding effect of  $\beta$ -CD-AOI might enable these unconventional adhesion properties, which are quite different from the results of HDDA. The decline of the peel strength at 0.20 mol % of  $\beta$ -CD-AOI (30.27 N/25 mm) originated from a failure-type transition of PSAs (Figure S13). The PSA- $\beta$ -CD-AOI showed cohesive failures until 0.15 mol %, signifying that the interfacial interactions are higher than the coherent strength. However, the failure type at 0.20 mol % was shifted to adhesive failure, meaning that the cohesive interactions become more considerable than the interfacial interactions. The decreased peel strength for the adhesive failure (at 0.20 mol %) is related to the restricted fibrillation of PSAs in the deformation process.<sup>47</sup>

The PSAs were characterized by a lap shear test to determine the difference in shear stress between the covalent and supramolecular cross-linking (Figure 1c-e). The shear strength was enhanced with the addition of HDDA, explaining the higher cohesive interactions with the increased cross-linking. However, it showed a critical decrease of shear displacement than the noncross-linked PSAs (pristine). The displacement for pristine was 8  $\mu$ m, but it was drastically decreased to 4  $\mu$ m for 0.5 mol % and 0.5  $\mu$ m for 0.20 mol % HDDA. The strict bonding between PSAs might hinder the movement of polymer chains, making the polymers hard to be stretched. On the other hand, the PSAs with a supramolecular cross-linker exhibited a completely similar displacement despite the increased cross-linking. Besides, the shear strength was improved more than 100% from 29.9 to 64.1 kPa with 0.20 mol % of  $\beta$ -CD-AOI. These unusual cross-linking behaviors would result from the sliding effect of  $\beta$ -CD-AOI, enhancing the shear strength without the compensation of chain

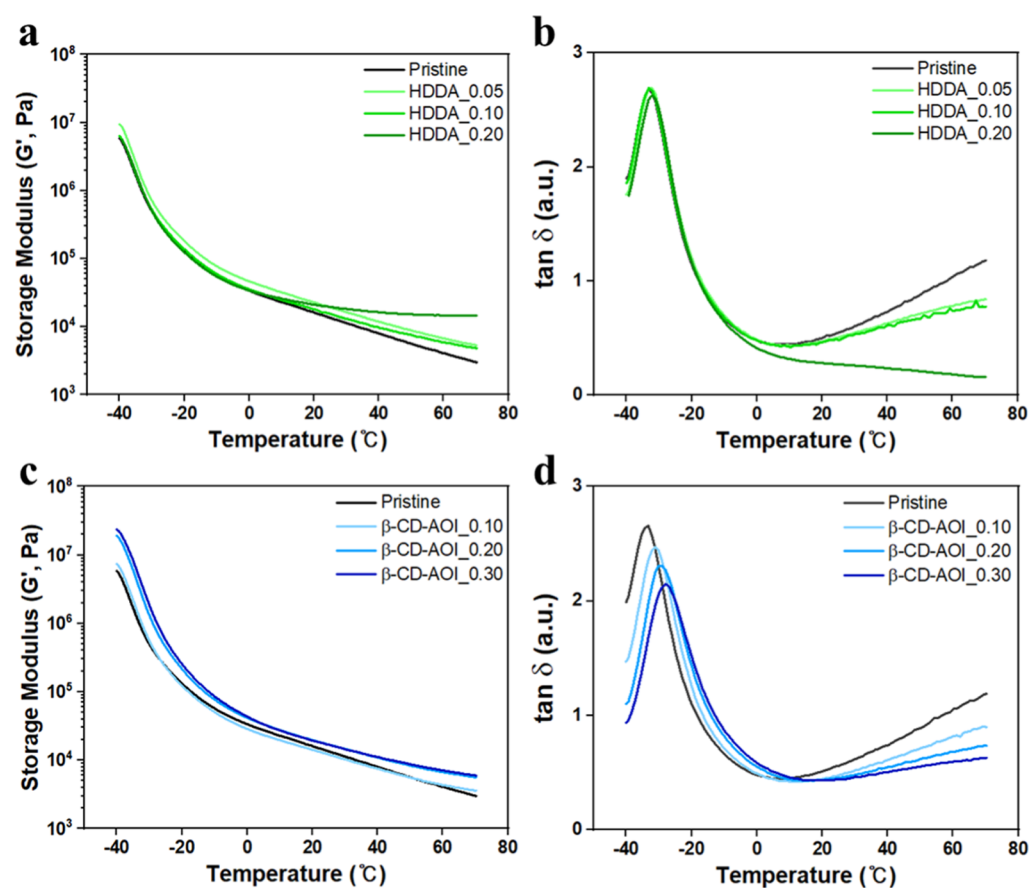


**Figure 3.** Storage modulus and loss factors ( $\tan \delta$ ) of the PSAs with (a,b) HDDDA and (c,d)  $\beta$ -CD-AOI with 1% strain over the temperature range of  $-40$  to  $70$   $^{\circ}\text{C}$ .

mobilities in polymers. Through the movable cross-linking of  $\beta$ -CD-AOI, we could overcome the limitation of cross-linking in adhesives.

The rheological properties and stress relaxation effects were investigated to identify the different cross-linkings between HDDDA and  $\beta$ -CD-AOI (Figures 3 and 4). The storage modulus of PSAs in temperature sweep tests did not present a specific change in the range from  $-40$  to  $70$   $^{\circ}\text{C}$  except for HDDDA\_0.20, which showed a clear increase in the storage modulus at  $20$  to  $70$   $^{\circ}\text{C}$  (Figure 3a). The glass-transition temperature ( $T_g$ ) for the pristine PSAs was  $-33$   $^{\circ}\text{C}$ , and it remained unchanged with the addition of HDDDA. In contrast, PSA  $\beta$ -CD-AOI showed an increased  $T_g$  proportionally to the cross-linker amount with lowered  $\tan \delta$ . The higher  $T_g$  for PSA  $\beta$ -CD-AOI might originate from the bulkier molecular structure of  $\beta$ -CD-AOI. The  $T_g$  of PSAs was also confirmed by DSC, and the results showed a similar tendency (Figure S14, Table S3). From the point of view of  $T_g$ , PSA  $\beta$ -CD-AOI should be less flexible than PSA HDDDA. However, it is not reasonable because  $\beta$ -CD-AOI showed higher stretching and adhesion properties than HDDDA in the adhesion test (Figure 2).

Thus, we additionally conducted frequency sweep tests for the PSAs with a shear rate of  $0.1$ – $100$  rad/s (Figure 4a,b). With the increase of the cross-linker, PSA HDDDA showed an apparent increase in the storage modulus with a critical reduction of loss factors ( $\tan \delta$ ). A strict network from a covalent cross-linking might be the reason for the transformation. On the other hand, PSA  $\beta$ -CD-AOI presented a

much higher  $\tan \delta$ , and the change of the storage modulus was not significant. Though the addition of  $\beta$ -CD-AOI showed higher  $T_g$ , PSA  $\beta$ -CD-AOI showed superior viscoelastic properties compared to PSA HDDDA in the frequency sweep test. Stress relaxation tests also confirmed the superior chain mobility of PSA  $\beta$ -CD-AOI (Figure 4c,d). The PSAs were attached between poly(methyl methacrylate) substrates and applied tensile stress to make a continuous shear strain (100%) for the stress relaxation tests. The stress at this condition was recorded to compare the relaxation effects of the PSAs. All specimens showed a time-dependent stress reduction, but the saturated values were significantly different according to their cross-linking states. PSA pristine showed a near-complete relaxation (95.7%), exhibiting its unrestricted chain mobility. However, PSA HDDDA showed a rapid decrease in the relaxation property from 83.1% (0.05 mol %) to 35.0% (0.20 mol %), giving an immense gap between 0.05 and 0.10 mol %. The gap of the relaxation ratio might originate from a fully connected network of PSAs over a concentration of 0.10 mol %, which prohibits polymer chain movement extensively. This result could be related to the probe tack properties, as shown in Figure 2b. The restrained chain mobility in PSAs hinders the wetting of adhesives causing poor tackiness.<sup>48</sup> Contrarily, the stress relaxation properties of PSA  $\beta$ -CD-AOI were retained considerably, even at a concentration of 0.30 mol % (78.1%). This high relaxation effect might be clear evidence of the sliding effect of  $\beta$ -CD-AOI, which negligibly hinders the chain mobility. From the results of rheological and stress relaxation tests, we could confirm that the supramolecular cross-linker

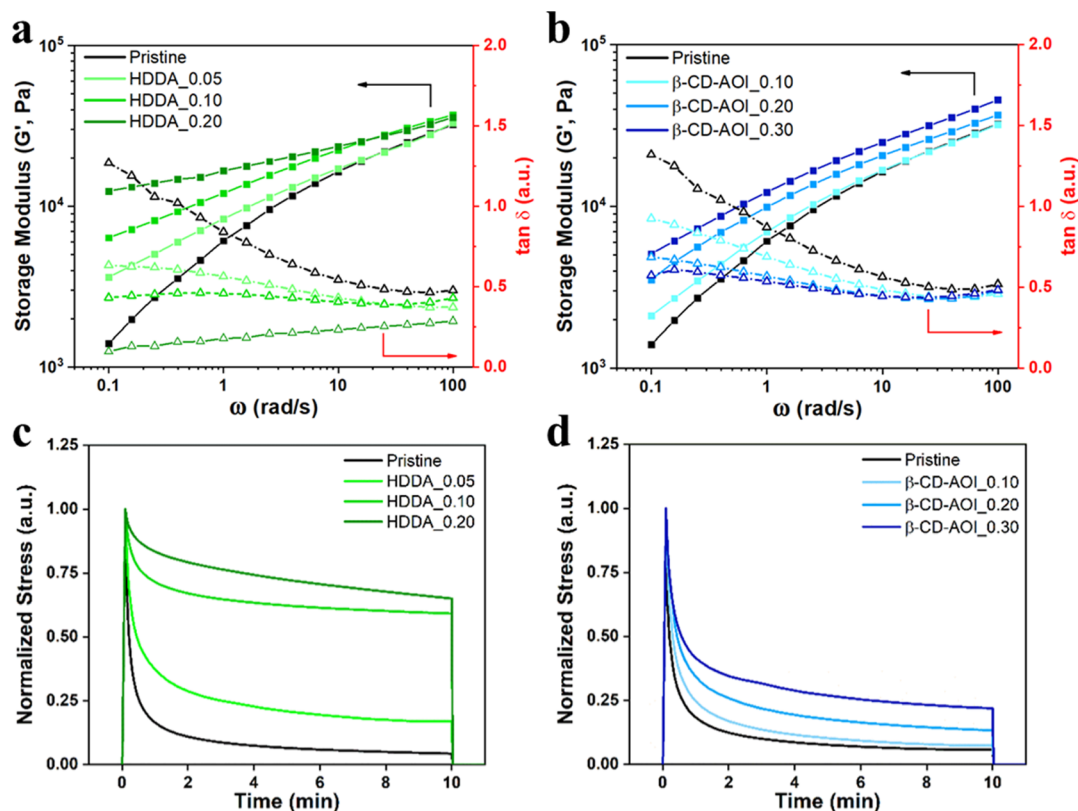


**Figure 4.** Rheological properties and stress relaxation effects of the PSAs. The storage modulus and loss factors ( $\tan \delta$ ) for (a) PSA\_HDDA and (b) PSA\_β-CD-AOI in rheological tests and the normalized stress of (c) PSA\_HDDA and (d) PSA\_β-CD-AOI in stress relaxation tests.

improves the cohesive interactions without the critical compensation of chain mobility via the sliding effect.

#### 4. CONCLUSIONS

In this study, we demonstrated that the acrylic functional group-modified β-CD (β-CD-AOI) could make a threaded compound with pBA, showing a supramolecular sliding effect in the polymer. The threading and sliding effect of pBA\_β-CD-AOI was confirmed by NOESY NMR and SAXS. The elastomers and PSAs with the supramolecular cross-linker showed exceptional stretching and adhesion properties, which are hard to obtain from a conventional cross-linker. The movability of the supramolecular cross-linker was characterized by rheological properties and stress relaxation tests. Especially, the PSAs with the supramolecular cross-linker retained their chain mobility despite the increase of the amount of cross-linking agent, overcoming the trade-off relationship of covalent cross-linking. This supramolecular cross-linker is expected to open a new paradigm of cross-linking for advanced polymers, which could widen human life advancement.

#### ■ ASSOCIATED CONTENT

##### Supporting Information

The Supporting Information is available free of charge at <https://pubs.acs.org/doi/10.1021/acsapm.1c00240>.

Image of the prepared elastomer; gel content of elastomers and PSAs; failure type of PSAs; rheological properties of PSAs; FT-IR spectra of materials; NMR spectra of the synthesized materials; and mass spectra (PDF)

Cycle test of elastomers (MP4)

#### ■ AUTHOR INFORMATION

##### Corresponding Author

Hyun-Joong Kim – Program in Environmental Materials Science, Department of Agriculture, Forestry and Bioresources and Research Institute of Agriculture and Life Sciences, Seoul National University, Seoul 08826, Republic of Korea; [orcid.org/0000-0002-7347-7534](https://orcid.org/0000-0002-7347-7534); Email: [hjokim@snu.ac.kr](mailto:hjokim@snu.ac.kr); Fax: +82 28732318

##### Authors

Mo-Beom Yi – Program in Environmental Materials Science, Department of Agriculture, Forestry and Bioresources, Seoul National University, Seoul 08826, Republic of Korea

Tae-Hyung Lee – Program in Environmental Materials Science, Department of Agriculture, Forestry and Bioresources, Seoul National University, Seoul 08826, Republic of Korea

Gi-Yeon Han – Program in Environmental Materials Science, Department of Agriculture, Forestry and Bioresources, Seoul National University, Seoul 08826, Republic of Korea

Hoon Kim – Program in Environmental Materials Science, Department of Agriculture, Forestry and Bioresources, Seoul National University, Seoul 08826, Republic of Korea;

[orcid.org/0000-0002-4447-4553](https://orcid.org/0000-0002-4447-4553)

Youngdo Kim – Samsung Display Co., Ltd., Cheonan 31086, Republic of Korea

Han-Sun Ryou – Samsung Display Co., Ltd., Cheonan 31086, Republic of Korea

Dong-Un Jin – Samsung Display Co., Ltd., Cheonan 31086, Republic of Korea

Complete contact information is available at:

<https://pubs.acs.org/doi/10.1021/acsapm.1c00240>

## Funding

This work was financially supported by Samsung Display Co., Ltd.

## Notes

The authors declare no competing financial interest.

## ACKNOWLEDGMENTS

We would like to thank Anton Paar Korea and Seol-Hee Jeon of Anton Paar Korea for their free support of rheological tests.

## REFERENCES

- (1) Wang, S.; Xu, J.; Wang, W.; Wang, G.-J. N.; Rastak, R.; Molina-Lopez, F.; Chung, J. W.; Niu, S.; Feig, V. R.; Lopez, J.; Lei, T.; Kwon, S.-K.; Kim, Y.; Foudeh, A. M.; Ehrlich, A.; Gasperini, A.; Yun, Y.; Murmann, B.; Tok, J. B.-H.; Bao, Z. Skin electronics from scalable fabrication of an intrinsically stretchable transistor array. *Nature* **2018**, *555*, 83–88.
- (2) Ling, Y.; An, T.; Yap, L. W.; Zhu, B.; Gong, S.; Cheng, W. Disruptive, soft, wearable sensors. *Adv. Mater.* **2020**, *32*, 1904664.
- (3) Li, L.; Lou, Z.; Chen, D.; Jiang, K.; Han, W.; Shen, G. Recent advances in flexible/stretchable supercapacitors for wearable electronics. *Small* **2018**, *14*, 1702829.
- (4) Liu, Y.; Fan, X.; Feng, W.; Shi, X.; Li, F.; Wu, J.; Ji, X.; Liang, J. An in situ and rapid self-healing strategy enabling a stretchable nanocomposite with extremely durable and highly sensitive sensing features. *Mater. Horiz.* **2021**, *8*, 250–258.
- (5) Seo, J.; Moon, S. W.; Kang, H.; Choi, B.-H.; Seo, J.-H. Foldable and Extremely Scratch-Resistant Hard Coating Materials from Molecular Necklace-like Cross-Linkers. *ACS Appl. Mater. Interfaces* **2019**, *11*, 27306–27317.
- (6) Jin, K.; López Barreiro, D.; Martin-Martinez, F. J.; Qin, Z.; Hamm, M.; Paul, C. W.; Buehler, M. J. Improving the performance of pressure sensitive adhesives by tuning the cross-linking density and locations. *Polymer* **2018**, *154*, 164–171.
- (7) Gent, A. N.; Tobias, R. H. Threshold tear strength of elastomers. *J. Polym. Sci., Polym. Phys. Ed.* **1982**, *20*, 2051–2058.
- (8) Back, J.-H.; Baek, D.; Sim, K.-B.; Oh, G.-Y.; Jang, S.-W.; Kim, H.-J.; Kim, Y. Optimization of Recovery and Relaxation of Acrylic Pressure-Sensitive Adhesives by Using UV Patterning for Flexible Displays. *Ind. Eng. Chem. Res.* **2019**, *58*, 4331–4340.
- (9) Czech, Z. Synthesis and cross-linking of acrylic PSA systems. *J. Adhes. Sci. Technol.* **2007**, *21*, 625–635.
- (10) Awaja, F.; Gilbert, M.; Kelly, G.; Fox, B.; Pigram, P. J. Adhesion of polymers. *Prog. Polym. Sci.* **2009**, *34*, 948–968.
- (11) Gu, Z.; Wan, X.; Lou, Z.; Zhang, F.; Shi, L.; Li, S.; Dai, B.; Shen, G.; Wang, S. Skin adhesives with controlled adhesion by polymer chain mobility. *ACS Appl. Mater. Interfaces* **2018**, *11*, 1496–1502.
- (12) Cordier, P.; Tournilhac, F.; Soulié-Ziakovic, C.; Leibler, L. Self-healing and thermoreversible rubber from supramolecular assembly. *Nature* **2008**, *451*, 977–980.
- (13) Fox, J.; Wie, J. J.; Greenland, B. W.; Burattini, S.; Hayes, W.; Colquhoun, H. M.; Mackay, M. E.; Rowan, S. J. High-strength, healable, supramolecular polymer nanocomposites. *J. Am. Chem. Soc.* **2012**, *134*, 5362–5368.
- (14) Sakai, T.; Matsunaga, T.; Yamamoto, Y.; Ito, C.; Yoshida, R.; Suzuki, S.; Sasaki, N.; Shibayama, M.; Chung, U.-i. Design and fabrication of a high-strength hydrogel with ideally homogeneous network structure from tetrahedron-like macromonomers. *Macromolecules* **2008**, *41*, 5379–5384.
- (15) Lee, S.; Hong, P. H.; Kim, J.; Choi, K.; Moon, G.; Kang, J.; Lee, S.; Ahn, J. B.; Eom, W.; Ko, M. J.; Hong, S. W. Highly Self-Healable Polymeric Blend Synthesized Using Polymeric Glue with Outstanding Mechanical Properties. *Macromolecules* **2020**, *53*, 2279–2286.
- (16) Cho, Y.; Kim, J.; Elabd, A.; Choi, S.; Park, K.; Kwon, T. W.; Lee, J.; Char, K.; Coskun, A.; Choi, J. W. A Pyrene-Poly(acrylic acid)-Polyrotaxane Supramolecular Binder Network for High-Performance Silicon Negative Electrodes. *Adv. Mater.* **2019**, *31*, 1905048.
- (17) Appel, E. A.; Biedermann, F.; Rauwald, U.; Jones, S. T.; Zayed, J. M.; Scherman, O. A. Supramolecular cross-linked networks via host–guest complexation with cucurbit [8] uril. *J. Am. Chem. Soc.* **2010**, *132*, 14251–14260.
- (18) Ahn, Y.; Jang, Y.; Selvapalam, N.; Yun, G.; Kim, K. Supramolecular velcro for reversible underwater adhesion. *Angew. Chem., Int. Ed.* **2013**, *52*, 3140–3144.
- (19) Yu, C.; Alkekha, D.; Shukla, A.  $\beta$ -Lactamase Responsive Supramolecular Hydrogels with Host–Guest Self-Healing Capability. *ACS Appl. Polym. Mater.* **2019**, *2*, 55–65.
- (20) Takashima, Y.; Sahara, T.; Sekine, T.; Kakuta, T.; Nakahata, M.; Otsubo, M.; Kobayashi, Y.; Harada, A. Supramolecular adhesives to hard surfaces: adhesion between host hydrogels and guest glass substrates through molecular recognition. *Macromol. Rapid Commun.* **2014**, *35*, 1646–1652.
- (21) Bin Imran, A.; Esaki, K.; Gotoh, H.; Seki, T.; Ito, K.; Sakai, Y.; Takeoka, Y. Extremely stretchable thermosensitive hydrogels by introducing slide-ring polyrotaxane cross-linkers and ionic groups into the polymer network. *Nat. Commun.* **2014**, *5*, 5124.
- (22) Sinawang, G.; Kobayashi, Y.; Osaki, M.; Takashima, Y.; Harada, A.; Yamaguchi, H. Mechanical and self-recovery properties of supramolecular ionic liquid elastomers based on host–guest interactions and correlation with ionic liquid content. *RSC Adv.* **2019**, *9*, 22295–22301.
- (23) Hou, J.-B.; Zhang, X.-Q.; Wu, D.; Feng, J.-F.; Ke, D.; Li, B.-J.; Zhang, S. Tough Self-Healing Elastomers Based on the Host-Guest Interaction of Polycyclodextrin. *ACS Appl. Mater. Interfaces* **2019**, *11*, 12105–12113.
- (24) Harada, A.; Kobayashi, R.; Takashima, Y.; Hashidzume, A.; Yamaguchi, H. Macroscopic self-assembly through molecular recognition. *Nat. Chem.* **2011**, *3*, 34–37.
- (25) Nomimura, S.; Osaki, M.; Park, J.; Ikura, R.; Takashima, Y.; Yamaguchi, H.; Harada, A. Self-Healing Alkyl Acrylate-Based Supramolecular Elastomers Cross-Linked via Host–Guest Interactions. *Macromolecules* **2019**, *52*, 2659–2668.
- (26) Nakahata, M.; Mori, S.; Takashima, Y.; Yamaguchi, H.; Harada, A. Self-Healing Materials Formed by Cross-Linked Polyrotaxanes with Reversible Bonds. *Chem* **2016**, *1*, 766–775.
- (27) Guo, K.; Zhang, D.-L.; Zhang, X.-M.; Zhang, J.; Ding, L.-S.; Li, B.-J.; Zhang, S. Conductive elastomers with autonomic self-healing properties. *Angew. Chem., Int. Ed.* **2015**, *54*, 12127–12133.
- (28) Li, Y.; Li, W.; Sun, A.; Jing, M.; Liu, X.; Wei, L.; Wu, K.; Fu, Q. A self-reinforcing and self-healing elastomer with high strength, unprecedented toughness and room-temperature reparability. *Mater. Horiz.* **2021**, *8*, 267–275.
- (29) Pazos, E.; Novo, P.; Peinador, C.; Kaifer, A. E.; García, M. D. Cucurbit[8]uril (CB[8])-Based Supramolecular Switches. *Angew. Chem., Int. Ed.* **2019**, *58*, 403–416.
- (30) Stupp, S. I.; LeBonheur, V.; Walker, K.; Li, L.-S.; Huggins, K. E.; Keser, M.; Amstutz, A. Supramolecular materials: self-organized nanostructures. *Science* **1997**, *276*, 384–389.
- (31) Courtois, J.; Baroudi, I.; Nouvel, N.; Degrandi, E.; Pensec, S.; Ducouret, G.; Chanéac, C.; Bouteiller, L.; Creton, C. Supramolecular Soft Adhesive Materials. *Adv. Funct. Mater.* **2010**, *20*, 1803–1811.
- (32) Heinzmann, C.; Weder, C.; de Espinosa, L. M. Supramolecular polymer adhesives: advanced materials inspired by nature. *Chem. Soc. Rev.* **2016**, *45*, 342–358.
- (33) Yamauchi, K.; Lizotte, J. R.; Long, T. E. Thermoreversible poly(alkyl acrylates) consisting of self-complementary multiple hydrogen bonding. *Macromolecules* **2003**, *36*, 1083–1088.
- (34) Cheng, S.; Zhang, M.; Dixit, N.; Moore, R. B.; Long, T. E. Nucleobase Self-Assembly in Supramolecular Adhesives. *Macromolecules* **2012**, *45*, 805–812.
- (35) Anderson, C. A.; Jones, A. R.; Briggs, E. M.; Novitsky, E. J.; Kuykendall, D. W.; Sottos, N. R.; Zimmerman, S. C. High-affinity DNA base analogs as supramolecular, nanoscale promoters of macroscopic adhesion. *J. Am. Chem. Soc.* **2013**, *135*, 7288–7295.

- (36) Nakamura, T.; Takashima, Y.; Hashidzume, A.; Yamaguchi, H.; Harada, A. A metal-ion-responsive adhesive material via switching of molecular recognition properties. *Nat. Commun.* **2014**, *5*, 4622.
- (37) Okumura, Y.; Ito, K. The polyrotaxane gel: A topological gel by figure-of-eight cross-links. *Adv. Mater.* **2001**, *13*, 485–487.
- (38) Choi, S.; Kwon, T. W.; Coskun, A.; Choi, J. W. Highly elastic binders integrating polyrotaxanes for silicon microparticle anodes in lithium ion batteries. *Science* **2017**, *357*, 279–283.
- (39) Wang, Z.; Ren, Y.; Zhu, Y.; Hao, L.; Chen, Y.; An, G.; Wu, H.; Shi, X.; Mao, C. A Rapidly Self-Healing Host-Guest Supramolecular Hydrogel with High Mechanical Strength and Excellent Biocompatibility. *Angew. Chem., Int. Ed.* **2018**, *57*, 9008–9012.
- (40) Zhang, L.; Cao, Y.; Wang, L.; Shao, L.; Bai, Y. Synthesis and properties of soap-free P (2-EHA-BA) emulsion for removable pressure sensitive adhesives. *RSC Adv.* **2014**, *4*, 47708–47713.
- (41) Gotoh, H.; Liu, C.; Imran, A. B.; Hara, M.; Seki, T.; Mayumi, K.; Ito, K.; Takeoka, Y. Optically transparent, high-toughness elastomer using a polyrotaxane cross-linker as a molecular pulley. *Sci. Adv.* **2018**, *4*, No. eaat7629.
- (42) Pruksawan, S.; Samitsu, S.; Yokoyama, H.; Naito, M. Homogeneously Dispersed Polyrotaxane in Epoxy Adhesive and Its Improvement in the Fracture Toughness. *Macromolecules* **2019**, *52*, 2464–2475.
- (43) Koyanagi, K.; Takashima, Y.; Yamaguchi, H.; Harada, A. Movable Cross-Linked Polymeric Materials from Bulk Polymerization of Reactive Polyrotaxane Cross-Linker with Acrylate Monomers. *Macromolecules* **2017**, *50*, 5695–5700.
- (44) Creton, C. Pressure-sensitive adhesives: an introductory course. *MRS Bull.* **2003**, *28*, 434–439.
- (45) Dahlquist, C. A. Pressure-sensitive adhesives. *Treatise Adhes. Adhes.* **1969**, *2*, 219–260.
- (46) Gent, A. N.; Schultz, J. Effect of wetting liquids on the strength of adhesion of viscoelastic material. *J. Adhes.* **1972**, *3*, 281–294.
- (47) Lakrout, H.; Sergot, P.; Creton, C. Direct observation of cavitation and fibrillation in a probe tack experiment on model acrylic pressure-sensitive-adhesives. *J. Adhes.* **1999**, *69*, 307–359.
- (48) Zosel, A. Effect of cross-linking on tack and peel strength of polymers. *J. Adhes.* **1991**, *34*, 201–209.